In compliance with the Wiley self-archiving policy:

This is the peer reviewed version of the following article: [Azmy, B., Standen, G., Kristova, P., Flint, A., Lewis, A. L. and Salvage, J. P. (2017), Nanostructured DPA-MPC-DPA triblock copolymer gel for controlled drug release of ketoprofen and spironolactone. Journal of Pharmacy and Pharmacology. doi: 10.1111/jphp.12733], which has been published in final form at [http://dx.doi.org/10.1111/jphp.12733]. This article may be used for non-commercial purposes in accordance with Wiley Terms and Conditions for Self-Archiving.

http://onlinelibrary.wiley.com/wol1/doi/10.1111/jphp.12733/abstract

Publication History
Submitted: 23rd January 2017
Accepted: 26th March 2017
Published Online: 7th May 2017

In accordance with the Wiley self-archiving policy, there is a 12 months embargo on this document.

Manuscript submitted to Journal of Pharmacy and Pharmacology
"Pharmaceutics and Drug Delivery"

Nanostructured DPA-MPC-DPA triblock copolymer gel for controlled drug release of ketoprofen and spironolactone

Bahaa Azmy[a], Guy Standen[a], Petra Kristova[a], Andrew Flint[a], Andrew L. Lewis[b], Jonathan P. Salvage[a]*

[a]University of Brighton, School of Pharmacy and Biomolecular Sciences, Huxley Building, Lewes Road, Brighton, BN2 4GJ, UK

[b]Biocompatibles UK Ltd, a BTG International plc group company, Innovation Group, Lakeview, Riverside Way, Watchmoor Park, Camberley, GU15 3YL, UK

*Corresponding Author
Dr Jonathan P. Salvage
University of Brighton
School of Pharmacy and Biomolecular Sciences
Huxley Building
Brighton, BN2 4GJ
UK.
E-mail: J.P.Salvage@brighton.ac.uk

Abstract

Objective

Uncontrolled rapid release of drugs can reduce their therapeutic efficacy and cause undesirable toxicity; however, controlled release from reservoir materials helps overcome this issue. The aims of this study were to determine the release profiles of ketoprofen and spironolactone from a pH-responsive self-assembling DPA-MPC-DPA triblock copolymer gel, and elucidate underlying physiochemical properties.

Methods

Drug release profiles from DPA_{50}-MPC_{250}-DPA_{50} gel (pH 7.5), over 32 hours (37 °C), were determined using UV-Vis spectroscopy. Nanoparticle size was measured by dynamic light scattering (DLS), and critical micelle concentration (CMC) by pyrene fluorescence. Polymer gel viscosity was examined via rheology, nanoparticle morphology investigated using scanning transmission electron microscopy (STEM), and the gel matrix observed using cryo-scanning electron microscopy (Cryo-SEM).

Key Findings

DPA_{50}-MPC_{250}-DPA_{50} copolymer (15 % w/v) formed a free-standing gel (pH 7.5) that controlled drug release relative to free drugs. The copolymer possessed a low CMC, nanoparticle size increased with copolymer concentration, and DLS data was consistent with STEM. The gel displayed thermostable viscosity at physiological temperatures, and the gel matrix was a nanostructured aggregation of smaller nanoparticles.

Conclusions

The DPA_{50}-MPC_{250}-DPA_{50} copolymer gel could be used as a drug delivery system to provide the controlled drug release of ketoprofen and spironolactone.

Keywords

DPA-MPC-DPA, pH sensitive, Nanoparticles, Polymer gel, Drug delivery system, Controlled release

Introduction

Traditional drug formulations for parenteral and oral administrations, can experience challenges such as rapid, first pass, metabolism where the drug is metabolised quickly in the liver before reaching the blood circulation, resulting in low efficacy and high side effects. Nanotechnology has afforded the development of pharmaceutical strategies to produce therapeutics with improved metabolism, dissolution and clearance profiles, and in doing so, reduce side effects and increase the efficacy of medicines. For example, nanoparticles have important advantages such as the surface area per unit mass of nano-sized formulations being significantly improved, leading to increased dissolution rates, however, intravenously administered therapeutic agents can also target healthy cells and create undesired side effects. [1]

An alternative strategy is available in the form of polymer gel biomaterials that can act as controlled release reservoirs, either at the site of localised therapeutic action, or as a depot for wider distribution in a controlled and extended mode, and thus reduce unwanted systemic effects. Recently there has been interest in stimuli-responsive block copolymer hydrogels with temperature [2, 3] and pH-responsive sensitivity [4 - 6] for pharmaceutical applications. These have included triblock copolymers containing both hydrophilic and hydrophobic domains for the formation of nanoparticle micelle based gels for drug delivery system applications, [7 - 10] where formation of free-standing hydrogels is achieved by a polymeric nanostructure. [11] Examples of proposed applications include suppositories, [12] implants, [13] and transdermal patches, [14] to provide controlled drug release at a target site, with Poloxamer based hydrogels often described. [15 – 17] The principle advantage of triblock ABA copolymers, for example PEG-PLGA-PEG over diblock AB copolymers, for example PEG-PLGA, being the ability of the triblock to form gels at a lower polymer concentration, [18] due to the B block forming bridges between the A blocks, [19] when in a solvent that is suitable for one of the blocks. [20]

For a drug-eluting biomaterial to be fit for purpose it needs to be biocompatible, and ideally biomimetic, such that it avoids eliciting an immune response at the host site which may negatively affect the drug elution kinetics. One strategy to achieve this is to mimic cell membrane components, and thus copolymers utilising phosphorylcholine (PC) have been developed for biomedical applications, [21, 22] including those that form hydrogels. [23 – 25] An example of PC containing polymers are the poly(2-methacryloyloxyethyl phosphorylcholine)-*b*-poly(2-(diisopropylamino)ethyl methacrylate) (MPC-DPA) range of diblock copolymers that have been developed for nanoparticle suspension drug delivery applications. [26 - 28] The MPC component is biocompatible and able to resist protein adsorption and cell adhesion, [29 – 31] due to high levels of water binding,

[32] however, the MPC-DPA diblock copolymers do not form gels. [4] In contrast, development and investigation of DPA-MPC-DPA triblock copolymers has, to date, been limited to a small number of reports. [4, 33 – 35]

The triblock copolymer DPA_{50}-MPC_{250}-DPA_{50} contains an MPC core block to provide biocompatibility, [32] and has been shown to form gels at concentrations above 10 % w/v at pH 7.5, [4] where it was used as a model drug delivery system with dipyridamole. These pH sensitive polymers reversibly self-assemble when the pH of their local environment is raised, [26] which provides some advantages over chemically cross-linked hydrogels for biomedical applications. [2] For example, the *in situ* sol-gel transition is reliant upon physical-cross linking [36] which also provides a delivery mechanism for controlling drug release, together with subsequent ease of rapid removal of the polymer if necessary *via* a simple pH reduction. [37] Whilst there could be widespread applications for these DPA-MPC-DPA copolymer gels, [12, 14, 38] there remains a number of physiochemical characteristics which may affect drug release profiles from these materials, including particle size, drug concentration, and possible material interactions, which require further elucidation.

For this current study, contrasting hydrophilic and hydrophobic model drugs, ketoprofen and spironolactone**,** respectively, were chosen, based on their successful use in a PEG-PLGA-PEG polymer gel study. [39] Ketoprofen is antipyretic, anti-inflammatory, and analgesic, and spironolactone is a potassium sparing diuretic used as an antihypertensive drug and also to treat Oedema in congestive heart failure. [40]

The aims of this study were to determine the release profiles of ketoprofen and spironolactone from a pH-responsive self-assembling nanostructured DPA_{50}-MPC_{250}-DPA_{50} triblock copolymer gel, and elucidate the underlying physiochemical properties of the gel. The novelty of this papers lies within the novel DPA-MPC-DPA triblock copolymer, which to date has seen limited publication and research data dissemination, the underpinning novel data pertaining to the copolymer physicochemical characterisation and performance presented herein, and the novel application of the copolymer for controlled and extended drug release, in both singular and combined drug loaded configurations. As such, this paper reports for the first time novel data regarding controlled drug release from this copolymer gel biomaterial over a 32 hour period, together with gel viscosity at physiological temperatures, and reveals the underlying nanostructured architecture of the copolymer gel matrix. In doing so, it makes an important contribution to furthering the understanding of DPA-MPC-DPA triblock copolymers, and highlights the potential use of the copolymer gel for controlled drug delivery applications.

Materials and methods

Materials

The poly(2-(diisopropylamino)ethyl methacrylate)-*b*-poly(2-methacryloyloxyethyl phosphorylcholine)-*b*-poly(2-(diisopropylamino)ethyl methacrylate) (DPA_{50}-MPC_{250}-DPA_{50}) triblock copolymer was supplied by Prof Steven Armes (University of Sheffield, UK) having been synthesised by atom transfer radical polymerisation (ATRP), as detailed previously. [4] Hydrochloric acid (HCl), sodium hydroxide (NaOH), ketoprofen (keto) (98%), spironolactone (spiro) (97%), pyrene (99%), phosphotungstic acid (PTA), and Tween 20 were purchased from Sigma Aldrich, UK. Phosphate buffered saline (PBS), 12-14 kDa MWCO dialysis tubing, methanol, and 0.22 µm syringe filters were purchased from Fisher Scientific, UK. Transmission electron microscopy (TEM) grids were purchased from Agar Scientific, UK.

NMR and GPC polymer characterisation

Block ratio composition and molecular weight of the received DPA_{50}-MPC_{250}-DPA_{50} copolymer were confirmed by ^{1}H nuclear magnetic resonance spectroscopy (NMR) and gel permeation chromatography (GPC) using protocols detailed previously. [28]

DPA-MPC-DPA polymer solutions

The DPA_{50}-MPC_{250}-DPA_{50} copolymer was dissolved in 0.1 M HCl, the pH raised with 3M NaOH, and the final volume adjusted with deionised water. Samples were prepared at 0.15 % w/v (1.5 mg ml^{-1}), 1.5 % w/v (15 mg ml^{-1}) and 15 % w/v (150 mg ml^{-1}) at pH 2.0 and pH 7.5.

Ketoprofen and spironolactone standard curves

The lambda max (λ max) for keto and spiro was determined in release medium (RM), consisting of phosphate buffered saline (PBS) (pH 7.5) containing 0.2 % w/w Tween 20 [39] using a Perkin Elmer Lambda 25 UV-Vis spectrophotometer. Standard curves for serial halving dilutions of keto and spiro, singularly and in combination, in RM, (100 µg ml^{-1}) were then constructed.

Ketoprofen and spironolactone free drug release

Keto was dissolved in 0.1 M HCl, the pH adjusted to pH 7.5 with 3 M NaOH, and the volume adjusted with deionised water to give a test concentration of 10 mg ml^{-1}. [39] Test sample volumes (2 ml) were transferred to 12-14 kDa MWCO dialysis tubing, sealed, and placed in 10 ml of RM (pH 7.5) at 37 °C, with 100 rpm magnetic

bar stirring, to begin free drug release. Thermally equilibrated (37 °C) 10 ml volumes of RM were used to replace the RM at hourly time intervals. Keto concentration in the RM samples was determined at the λ max (260 nm) using the standard curve, and the cumulative release of free keto over 32 hours calculated. Spiro was prepared, and free drug release determined at the λ max (241 nm), as per keto, at a spiro test concentration of 2.5 mg ml^{-1}. [39] The free drug release over 32 hours for a combined sample of keto (10 mg ml^{-1}) and spiro (2.5 mg^{-1}) was also determined using the same methodology. Samples were prepared and measured in triplicate.

Ketoprofen and spironolactone controlled release from DPA-MPC-DPA gel

Keto loaded copolymer gel was prepared by dissolving DPA_{50}-MPC_{250}-DPA_{50} and keto in 0.1 M HCl, adjusting the pH to pH 7.5 with 3 M NaOH, to induce copolymer gelation, then adjusting the volume with deionised water to produce a 15 % w/v copolymer gel (150 mg ml^{-1}) containing keto at 10 mg ml^{-1}. Test sample volumes (2 ml) were transferred to 12-14 kDa MWCO dialysis tubing, sealed, and placed in 10 ml of RM (pH 7.5) at 37 °C, with 100 rpm magnetic bar stirring, to begin drug release. Thermally equilibrated (37 °C) 10 ml volumes of RM were used to replace the RM at hourly time intervals. Keto concentration in the RM samples was determined at the λ max (260 nm) using the standard curve, and the controlled cumulative release of keto from the 15 % w/v copolymer gel over 32 hours calculated. Spiro in 15 % w/v copolymer gel was prepared, and controlled drug release determined at the λ max (241 nm), as per keto, at a spiro concentration of 2.5 mg ml^{-1}. The controlled drug release over 32 hours for a combined sample of keto (10 mg ml^{-1}) and spiro (2.5 mg ml^{-1}) in 15 % w/v polymer gel was also determined using the same methodology. Samples were prepared and measured in triplicate.

Fourier transform infrared spectroscopy

Fourier transform infrared spectroscopy (FTIR) was performed on dried samples using a Perkin Elmer Spectrum 65 FT-IR spectrometer. All transmission spectra were obtained at ambient temperature by recording the average of 16 scans in the region between a wave number 4000 and 650 cm^{-1} with a resolution of 4 cm^{-1}.

Nanosystem characterisation

The DPA_{50}-MPC_{250}-DPA_{50} nanosystems were assessed for particle size, polydispersity, critical micelle concentration (CMC), viscosity, and particle morphology, using dynamic light scattering (DLS), fluorescence

spectrophotometry, rheology, scanning transmission electron microscopy (STEM), and cryo-scanning electron microscopy (Cryo-SEM).

Dynamic light scattering

Particle size (D_h) and polydispersity (Pd) of 0.15 % w/v solution DPA_{50}-MPC_{250}-DPA_{50} copolymer nanoparticle systems, at pH 2.0 and pH 7.5, were measured at 25° C, with a Malvern Zetasizer Nano ZS90 instrument, using the DLS method detailed previously. [28] Samples were prepared and measured in triplicate.

Critical micelle concentration

The CMC of the 1.5 % w/v DPA_{50}-MPC_{250}-DPA_{50} copolymer nanosystem at pH 7.5 was determined *via* fluorescence spectrometry using pyrene as the probe. Serial halving dilutions (3 ml volumes) of the sample were prepared with PBS (pH 7.5), and pyrene (25 µg ml^{-1} in methanol) added (50 µl) to each. The pyrene fluorescence spectra was measured for each dilution using a Varian Eclipse Fluorescence spectrophotometer, at an excitation wavelength of 334 nm, with emission collected from 345 – 480 nm, using 10 nm excitation and 2.5 nm emission slits, 30 nm min^{-1} scan rate, and 0.5 nm data interval. [41] Samples were prepared and measured in triplicate.

Rheology

The viscosity of the DPA_{50}-MPC_{250}-DPA_{50} copolymer nanosystems (0.15, 1.5, and 15 % w/v) at pH 7.5 was determined with a HAAKE Rheostress rheometer, using 1 Pa oscillating shear stress across a 20 – 50 °C temperature range at 1.5 °C intervals. Samples were prepared and measured in triplicate.

Scanning transmission electron microscopy

Particle morphology of 0.15 and 1.5 % w/v DPA_{50}-MPC_{250}-DPA_{50} copolymer nanoparticle systems was investigated at pH 7.5, *via* STEM, using a Zeiss SIGMA field emission gun scanning electron microscope (FEG-SEM) equipped with a Zeiss STEM detector. Working conditions used were; 20 kV accelerating voltage, 20 µm aperture, and 3 mm working distance. To prepare the STEM samples, 200 mesh Formvar coated copper TEM grids were plasma treated (5 watts) in a Polaron PT7150 plasma barrel etcher for 30 seconds, to improve surface wettability, 1 drop of sample applied to the TEM grid for 60 seconds, excess wicked way, 1 drop of filtered (0.22 µm) 2 % w/v PTA (pH 7.5) applied to the TEM grid for 60 seconds, excess wicked away, and then air dried.

Cryo scanning electron microscopy

The morphology of the 15 % w/v DPA_{50}-MPC_{250}-DPA_{50} copolymer nanoparticle system in gel form (pH 7.5), was examined via Cryo-SEM, using a Quorum Technologies PP3000T cryogenic sample preparation system and Zeiss SIGMA FEG-SEM, according to the method detailed previously. [28]

Data analysis

Data are presented as Mean ± standard deviation (SD) of triplicate repeat experiments (n = 3). The FDA preferred model-independent similarity factor, f_2, was calculated for comparing the cumulative release profiles where $f_2 > 50$ indicates similarity, and $f_2 = 100$ is considered identical. [42, 43] Model-dependant analysis of the release profiles was undertaken using zero order, first order, and Higuchi mathematical functions to determine the coefficient of determination R^2 values, where $R^2 >$ was indicative of good fit, and the rate constants K_0, K_1, and K_H respectively. [44, 45] Statistical significance of the cumulative release data was assessed using the non-parametric, two-tail, Mann-Whitney *U* test (Minitab 16), comparing the gel loaded drug release profile curves against the free drug release profile curves [46, 47] where $P < 0.05$ was considered significant.

Results and Discussion

NMR and GPC polymer characterisation

The composition of the DPA_{50}-MPC_{250}-DPA_{50} triblock copolymer was confirmed using ^{1}H NMR and GPC, as shown in Figure 1 and Table 1. The ^{1}H NMR data was consistent with previous reports, [4] whilst the GPC analysis, using an optimised organic GPC protocol, [28] improved the GPC to NMR data correlation. The results (Figure 1 and Table 1) indicated that the DPA_{50}-MPC_{250}-DPA_{50} copolymer was well defined, and of low polydispersity (1.01).

DPA-MPC-DPA polymer solutions

The DPA_{50}-MPC_{250}-DPA_{50} triblock copolymer aqueous solutions prepared (0.15, 1.5, and 15 % w/v) were fluid and free-flowing in acidic solution (pH 2). The pKa of DPA is circa pH 6, at which point it becomes deprotonated and hydrophobic [4], and diblock MPC-DPA copolymers are reported to form micelles between pH 6 and pH 7 in solution [26]. Therefore the DPA-MPC-DPA triblock copolymer is predicted to begin forming flower-like micelles across the same pH 6-7 range, with a resultant gel formation if the polymer w/v % is sufficient. When the pH was raised to pH 7.5, the 0.15 and 1.5 % w/v solutions remained free-flowing, whilst the

15 % w/v solution formed a free-standing gel, as seen in Figure 2. This was consistent with previous reports, [4] and attributed to the deprotonation of the DPA blocks resulting in micelle formation, and then subsequent interaction of the triblock chains to form the gel network observed at 15 % w/v concentration.

Ketoprofen and spironolactone standard curves

The λ max wavelengths for keto and spiro in RM were determined as 260 and 241 nm respectively, which were consistent with other reports. [39] Standard curves for these were constructed alone and in combination, as shown in Figure 3, with the coefficient of determination (R^2) values for all of curves (Figure 3 a, b, c, d) being 0.9996 or greater, and thus of good linear fit. These curves were subsequently used to determine the keto and spiro drug release profiles.

Ketoprofen and spironolactone individual release rates

Initially, keto and spiro were tested individually, and Figure 4 displays the free drug release, together with controlled release from the 15 % w/v DPA_{50}-MPC_{250}-DPA_{50} triblock copolymer gel, at pH 7.5 in RM. The keto (10 mg ml^{-1}) free drug release rate was rapid, with circa 82 % released after 1 hour, whilst in comparison, the DPA_{50}-MPC_{250}-DPA_{50} gel loaded keto displayed a decreased release rate of circa 58% at the 1 hour time point, a reduction of circa 24 %. The first 8 hours produced the greatest decrease in drug release, and controlled release of keto from the copolymer gel was maintained for the 32 hour experimental duration. The model-independent f_2 similarity value was calculated as 47, which was below the lower limit of the 50 to 100 similarity value range, and therefore the profiles were not considered similar. The Mann-Whitney *U* test indicated a statistically significant difference between the keto release profile curve from the copolymer gel (Median = 92.43) and the free keto release (Median = 97.41), W = 3435, p = 0.0025. The spiro (2.5 mg ml^{-1}) release rate was also decreased when loaded into the copolymer gel compared to the free drug, with a decrease in release rate from circa 16 % down to circa 10 % at the first hour, a reduction of circa 6 %, and again controlled release from the copolymer gel was maintained for the 32 hour experimental duration. The f_2 similarity value was calculated as 25, and therefore the profiles were not considered similar. The Mann-Whitney *U* test indicated a statistically significant difference between the spiro release profile from the copolymer gel (Median = 32.50) and the free spiro release (Median = 42.41), W = 3335, p = 0.0161. The difference between the keto and spiro release rates being primarily due to the hydrophilic nature of keto *versus* the hydrophobic nature of spiro. [39, 40] Indeed, keto has a carboxyl group which at pH 7.5 becomes ionized and hydrophilic, [39] whilst in contrast spiro is

hydrophobic, and thus the water solubility of keto has been reported as circa 135 mg ml^{-1} at pH 6, whereas sprio is considered insoluble in water. [39, 48] Therefore adding Tween 20 to the RM was required to improve the solubility of the drugs, in particular spiro, as the solubility of spiro in RM has been reported as 0.12 mg ml^{-1}. [39] Additionally, to ensure release of the drugs through the dialysis membrane a 12-14 kDa MWCO was chosen, which was greater than the molecular weights of spiro (0.42 kDa) and keto (0.25 kDa), and also lower than molecular weight (95 kDa) of the DPA_{50}-MPC_{250}-DPA_{50} copolymer to ensure it was retained within the membrane. As stated, the release medium used for the dialysis experimental work included Tween 20 at 0.2 % w/v, which has been shown to be effective for use in spiro and keto dialysis release models [39], and no precipitation of drugs was observed.

The difference in hydrophobicity between keto and spiro will have resulted in the drugs partitioning to different domains within the micelle based copolymer hydrogel, and thus the differing release profiles observed, which were consistent with previous keto and spiro data. [39] The model-dependant analysis of the keto, with and without gel, release data (Table 2) over the 0 – 32 hour time period indicated that zero order was not a good fit, with coefficient of determination R^2 values < 0.35 evident. First order was a closer fit for 0 - 32 hours, with R^2 values > 0.72, suggesting a concentration gradient related release of the hydrophilic keto. However it was also noted that the release rate was greater, and the slope steeper, within the first 0 – 8 hours relative to the final 24 – 32 hours (Figure 4), and thus possibly a biphasic release profile, comprising first order for 0 – 8 hours (R^2 > 0.84) and zero order for 24 – 32 hours (R^2 > 0.96). There was also some evidence for Higuchi model release (R^2 = 0.87) for the gel loaded keto sample during the 0 – 8 hour period, which would be consistent with the gel providing controlled diffusion and release of the keto. Comparison of the 0 – 8 hours first order rate constant (K_1) values (Table 2) indicated that gel loaded keto (K_1 = -0.124) was released at a slower rate than the free keto (K_1 = -0.189). The model-dependant analysis of the spiro, with and without gel, release data (Table 2) was similar to the keto release, with the data again suggesting a biphasic release of first order from 0 – 8 hours (R^2 > 0.88) followed by zero order for the 24 – 32 hour period (R^2 > 0.99), and also, again, possibly Higuchi release (R^2 > 0.91) due to gel loading and the hydrophobicity of spiro producing a matrix diffusion-like release profile. It has been reported previously that keto and spiro release from polymer gels may indeed fit first order and Higuchi models. [39] Comparison of the 0 – 8 hours first order rate constant (K_1) values (Table 2) indicated that gel loaded spiro (K_1 = -0.019) was released at a slower rate than the free spiro (K_1 = -0.024).

In summary, sustained and controlled drug release from the DPA_{50}-MPC_{250}-DPA_{50} 15 % w/v copolymer gel was achieved for keto and spiro relative to the free drugs. Whilst this current study investigated drug release at pH

7.5, and achieved reduced and controlled drug release profiles, reductions in the local pH environment could affect the profiles. If the pH was lowered the micelle based gel would dissociate and dissemble, which would result in a faster release of the loaded drugs, as reported previously [4] for dipyridamole release. Thus, given the pH responsive nature of the DPA-MPC-DPA polymer, [4] it also offers the possibility to react, and release drugs, to changes in localised pH, for example biofilm, [49] and tissue necrosis, [50] associated acidification, and thus respond actively and autonomously to changing therapeutic needs.

Ketoprofen and spironolactone combined release rates

Subsequently, the release rates for combinations of keto and spiro, as free drugs, and loaded into 15 % w/v DPA_{50}-MPC_{250}-DPA_{50} copolymer gels, were determined. It can be seen from Figure 5 and Table 3 that the combination release rate was reduced for the gel loaded drugs in comparison to the free drugs. Loading the keto and spiro together, in combination, in the copolymer gel produced a large decrease in keto release, from circa 71 % down to circa 32%, a reduction of circa 39 % at 1 hour, and also an overall decrease and prolonged controlled release for spiro over the 32 hour experimental time course. The model-independent f_2 similarity value for keto in combination with spiro was calculated as -13, and therefore the profiles were not considered similar. The Mann-Whitney *U* test indicated a statistically significant difference between the keto release profile from the copolymer with spiro gel (Median = 45.79) and the free keto with spiro release (Median = 97.91), W = 4370, $p < 0.001$. The f_2 similarity value for spiro in combination with keto was calculated as -4, and therefore the profiles were not considered similar. The Mann-Whitney *U* test indicated a statistically significant difference between the spiro release profile from the copolymer with keto gel (Median = 26.14) and the free spiro with keto release (Median = 57.94), W = 4109, $p < 0.001$.

Model-dependant analysis of the keto in combination with spiro, with and without gel, release data (Table 2) indicated that zero order was not an appropriate model ($R^2 < 0.40$) for the 0 – 32 hour period, and that the best fit for the profiles were first order during 0 – 8 hours ($R^2 > 0.75$) followed by zero order for 24 – 32 hours ($R^2 > 0.96$), and thus further evidence of biphasic release. The data (Table 2) also suggested, again, the possibility of Higuchi, matrix diffusion, release for the gel loaded sample ($R^2 = 0.90$) from 0 – 8 hours. Comparison of the 0 – 8 hrs first order rate constant (K_1) values (Table 2) indicated that gel loaded keto in combination with spiro ($K_1 = -0.035$) was released at a slower rate than the free keto in combination with spiro ($K_1 = -0.177$).

The spiro in combination with keto, without gel, also appeared to display biphasic release, with either first order ($R^2 = 0.92$) or Higuchi release ($R^2 = 0.96$), 0 – 8 hours, followed by zero order ($R^2 = 0.99$) over 24 – 32 hours.

Interestingly, the R^2 data for spiro in combination with keto, with gel loading, suggested that this sample underwent Higuchi release (R^2 = 0.88) followed by zero order (R^2 = 0.83) for the 0 – 8 and 24 – 32 hour periods respectively, possibly due to the combined effects of spiro hydrophobicity, material interactions, and gel loading, to create matrix diffusion-like release conditions. Comparison of the 0 – 8 hours first order rate constant (K_1) values (Table 2) indicated that gel loaded spiro in combination with keto (K_1 = -0.014) was released at a slower rate than the free spiro in combination with keto (K_1 = -0.042).

It is recognised that in some instances and applications, it may be expected or desirable, to control and achieve a full 100 % drug release over a set and distinct period of time. However, in the case of novel applications of newly emerging materials such as DPA-MPC-DPA, where "model" drugs are used for proof of concept, a set time is less relevant, as it may be the case that the controlled release is extended beyond the experimental period, as was observed with the 32 hours duration of this study. In doing so, the study and novel data provided an important insight into the potential for the material to be utilised as a reservoir for long-term, slow, zero order, drug release applications, for which future work is required to elucidate this further. For example, the elution test parameters can control the release profile, if more Tween 20 surfactant had been added to the RM, or a larger RM volume used, then the release profile would change, and, moreover, if lower amounts of drugs had been added to the gel, the cumulative % amount released would have been greater for the same 32 hour time period.

Regarding the slow release observed, the hydrophobic spiro would have partitioned into the flower-like micelle cores of the copolymer gel, due to the hydrophobic effect, whilst the more hydrophilic keto would have undergone molecular dissolution into the aqueous phase of the hydrated gel. The FTIR analysis suggested that there were no direct material interactions involved in controlling drug release; therefore the spiro in the micelle cores may have caused micelle driven gel constriction and restricted keto release, whilst the keto in the aqueous phase may have retarded the spiro release. The release profile slopes of the gel loaded drugs had indeed become shallow at 32 hours, but had not stopped, and over an extended period of time, which could be tuned and optimised to specific application needs, drug release would reach completion.

In summary, whilst the combined drug release profiles (Figure 5) differed from the individual drug release profiles (Figure 4), as summarised for the 1, 8, 24, and 32 hour time points in Table 3 and illustrated by the differing rate constant values in Table 2, the controlled drug release from the DPA_{50}-MPC_{250}-DPA_{50} 15 % w/v copolymer gel was again achieved relative to the free drugs.

Fourier transform infrared spectroscopy

It was noted from Figures 4 and 5, and Table 3 that the drug release profiles for keto and spiro altered when tested in combination *versus* when tested individually, and keto has been reported to undergo hydrogen bonding physical interactions with PLGA. [51] To explore this, FTIR was utilised to investigate possible polymer-drug and drug-drug interactions. However, in this instance, there was no evidence of sample material interactions, as there were no shifts in the characteristic absorbance peaks detectable in FTIR spectra, which are displayed in Figure 6. It is possible that the presence of the more hydrophobic spiro within the micelle cores caused the nanostructed gel to constrict, and thus reduced the keto release. Inversely, the more hydrophilic keto may have saturated the aqueous component of the gel, and thus retarded spiro release. The alterations in drug release profiles observed therefore require further investigation to be fully understood, and it has been suggested that inclusion of hydrophilic additives with hydrophobic drugs can indeed improve their water solubility. [52]

Dynamic light scattering

The DLS particle sizing data for DPA_{50}-MPC_{250}-DPA_{50} (0.15 % w/v) is shown in Table 4, and indicated that at pH 2.0 the particle size was circa 16 nm, which was consistent with unimer size, whilst at pH 7.5 the average particle size was circa 63 nm, which was indicative of micelle formation. [26] The polydispersity (Pd) of the samples was also reduced at pH 7.5, compared to pH 2.0, suggesting further the formation of uniform nano-structured morphologies. The DLS particle size data was in good agreement with the STEM imaging data.

Critical micelle concentration

The CMC of the DPA_{50}-MPC_{250}-DPA_{50} (1.5 % w/v) copolymer solutions (pH 7.5) was determined by pyrene fluorescence spectroscopy. The convention for determining CMC is to identify the points of inflection associated with spectral shifts in the pyrene fluorescence ratio for peaks 1 *vs* 3, [41, 53] resulting from changes in nanoparticle morphology. The morphological changes and spectral shifts are associated with the concentration dependant formation of micelles. [54 – 57] This can be seen in Figure 7, where the shift from unimer to micelle began at circa 0.004 mg ml^{-1} (CMC^1), and was complete by circa 0.469 mg ml^{-1} (CMC^3). Single values are often cited when reporting CMC data, however CMC can also be viewed as a concentration range, [58] with a start (CMC^1), mid (CMC^2), and end point (CMC^3), as highlighted in Figure 7, and thus herein the CMC range data are presented in Table 4.

With regard to the DPA-MPC-DPA copolymer, the hydrophilic MPC blocks surround the hydrophobic DPA blocks, and the DPA core of the micelle solubilizes the hydrophobic pyrene such that it acts as a precise probe

for the micelle formation process. [59 - 62] The CMC is an important parameter for improving dilution stability of the gel, decreasing the CMC improves micelle stability, and thus drug release is slower. [10]

Rheology

The viscosity (Pa.s) against temperature (20 – 50 °C) was determined for the 15, 1.5, and 0.15 % w/v solutions (pH 7.5) of DPA_{50}-MPC_{250}-DPA_{50} as shown in Figure 8. The rheological data was consistent with the 15 % w/v solution having formed a free-standing gel, as the viscosity ranged from circa 26 Pa.s at 20 °C to circa 43 Pa.s at 50 °C, suggesting some evidence of thermal-induced gel thickening from circa 40 – 50 °C. At physiological temperatures (36.5 – 37.5 °C) viscosity was circa 31 Pa.s, which was an improvement upon reports of other PC containing triblock copolymer gel systems, such as PPO-PMPC-PNIPAM, that had low viscosity (circa 1 Pa.s) across the same temperature range. [36] In contrast, the viscosity of the 1.5 and 0.15 % w/v solutions remained stable at, and less than, 0.01 Pa.s across the tested temperature range, which was consistent with the free-flowing solutions observed. In this study the gel was tested at 15 % w/v, and temperature induced gel transitions were observed between 40 – 50 °C. It has previously been reported that the gel consistency, and free-standing ability, increases as the % w/v increases [4]. Therefore it is possible that DPA-MPC-DPA gels prepared at much higher w/v % concentrations may indeed display a greater level of thermo-stability, and thus reduced level of sol-gel transitions at higher temperatures. In summary, the 15 % w/v DPA_{50}-MPC_{250}-DPA_{50} copolymer gel displayed stable viscosity at the physiological temperatures required for clinical application.

Scanning transmission electron microscopy

STEM imaging was conducted to investigate nanoparticle self-assembly, and morphology, of DPA_{50}-MPC_{250}-DPA_{50} copolymer at 0.15 and 1.5 % w/v solutions (pH 7.5). The 15 % w/v sample was in gel form, and not suitable for STEM analysis. As shown in Figure 9a and b, the 0.15 % w/v sample formed relatively uniform nanoparticles of circa 60 nm diameter, which was in close agreement with the DLS data (Table 4). The 1.5 % w/v sample formed larger flower-like particle aggregates of the smaller (60 nm) particles, which were circa 600 nm diameter, as seen in Figure 9c and d. These data supported the proposed, concentration dependant particle interaction, process responsible for driving the nanostructured gel formation. [4] Indeed, particle morphology changes have been reported previously for MPC-DPA diblock copolymers, [63, 64] and also alternative polymers, such as G54-H140 diblock copolymer, [11] where free-flowing spherical micelle solutions were reported at low concentration and free-standing wormlike micelle gels at high concentration.

Cryo scanning electron microscopy

The DPA_{50}-MPC_{250}-DPA_{50} bulk material gel matrix, and nano-morphology, of the 15 % w/v copolymer gel sample (pH 7.5) was examined using Cryo-SEM as seen in Figure 10. The results indicated that the bulk gel material consisted of an interconnected copolymer network matrix (Figure 10a), which was constructed from an aggregation of smaller nanoparticles of circa 60 nm diameter (Figure 10b). The triblock nanoparticle size and morphology was similar to previous reports of MPC-DPA diblock nanoparticles. [26 - 28, 63] The data were consistent with the DLS particle sizing (Table 4) and STEM imaging data (Figure 9), and illustrated further the concentration driven particle aggregation, at pH 7.5, proposed for the formation of the DPA_{50}-MPC_{250}-DPA_{50} nanostructured gel observed (Figure 10).

Conclusions

In conclusion, this paper presents the first report of keto and spiro loading and controlled release from the PC containing biomaterial triblock copolymer DPA_{50}-MPC_{250}-DPA_{50} gel system. The study contributed novel data to, and expanded upon, the currently limited knowledge of DPA-MPC-DPA, including an optimised GPC analysis, which provided an improved GPC to NMR correlation. The data successfully demonstrated controlled release of contrasting hydrophobic and hydrophilic drugs from a 15 % w/v gel over a 32 hour period, the potential to modulate release further by combining drugs, and the excellent stability of the gel in the form of physiologically thermostable viscosity and a low CMC. Investigation of the gel system architecture using STEM and Cryo-SEM revealed the concentration and pH driven nanoparticle aggregation, which resulted in formation of the nanostructured copolymer gel matrix. These novel data make an important contribution to elucidating the potential for pharmaceutical applications of DPA-MPC-DPA, and demonstrated the possibility of combinational drug therapy, which could provide treatment for several conditions from a single application.

Acknowledgements

The authors gratefully acknowledge Biocompatibles UK Ltd for provision of MPC, and Prof Steven Armes (University of Sheffield, UK) for supplying the test polymer.

References

1. Schoener CA, Hutson HN, Peppas NA. pH-responsive hydrogels with dispersed hydrophobic nanoparticles for the delivery of hydrophobic therapeutic agents. *Polymer International* 2012; 61(6): 874-879.
2. Li C, Tang Y, Armes SP, Morris CJ, Rose SF, Lloyd AW, et al. Synthesis and characterization of biocompatible thermo-responsive gelators based on ABA triblock copolymers. *Biomacromolecules* 2005; 6(2): 994-999.
3. Madsen J, Armes SP, Lewis AL. Preparation and aqueous solution properties of new thermoresponsive biocompatible ABA triblock copolymer gelators. *Macromolecule*. 2006; 22(39): 7455-7457.
4. Ma Y, Tang Y, Billingham NC, Armes SP, Lewis AL. Synthesis of biocompatible, stimuli-responsive, physical gels based on ABA triblock copolymers. *Biomacromolecules* 2003; 4(4): 864-868.
5. Chung HJ, Park TG. Self-assembled and nanostructured hydrogels for drug delivery and tissue engineering. *Nano Today* 2009; 4(5): 429-437.
6. He C, Kim SW, Lee DS. In situ gelling stimuli-sensitive block copolymer hydrogels for drug delivery. *Journal of controlled release* 2008; 127(3): 189-207.
7. Jeong B, Bae YH, Kim SW. Biodegradable thermosensitive micelles of PEG-PLGA-PEG triblock copolymers. *Colloids and Surfaces B: Biointerfaces* 1999; 16(1): 185-93.
8. Yokoyama M, Kwon GS, Okano T, Sakurai Y, Seto T, Kataoka K. Preparation of micelle-forming polymer-drug conjugates. *Bioconjugate chemistry* 1992; 3(4): 295-301.
9. Kwon GS, Naito M, Yokoyama M, Okano T, Sakurai Y, Kataoka K. Physical entrapment of adriamycin in AB block copolymer micelles. *Pharmaceutical research* 1995; 12(2): 192-195.
10. Kabanov AV, Nazarova IR, Astafieva IV, Batrakova EV, Alakhov VY, Yaroslavov AA, et al. Micelle formation and solubilization of fluorescent probes in poly (oxyethylene-b-oxypropylene-b-oxyethylene) solutions. *Macromolecules* 1995; 28(7): 2303-2314.
11. Blanazs A, Verber R, Mykhaylyk OO, Ryan AJ, Heath JZ, Douglas CWI, et al. Sterilizable gels from thermoresponsive block copolymer worms. *Journal of the American Chemical Society* 2012; 134(23): 9741-9748.
12. Özgüney I, Kardhiqi A. Properties of bioadhesive ketoprofen liquid suppositories: preparation, determination of gelation temperature, viscosity studies and evaluation of mechanical properties using

texture analyzer by 4× 4 factorial design. *Pharmaceutical development and technology* 2014; 19(8): 968-975.

13. Cheng F, Maggie JM, Ko Y-J, Lin M-Y, Shuen-Hsiang C. Recipe for in-situ gel, and implant, drug delivery system formed thereby. US Patents; US20150111834 A1, 2014.
14. Mavuso S, Marimuthu T, E Choonara Y, Kumar P, C du Toit L, Pillay V. A review of polymeric colloidal nanogels in transdermal drug delivery. *Current pharmaceutical design* 2015; 21(20): 2801-2813.
15. Fults KA, Johnston TP. Sustained-release of urease from a poloxamer gel matrix. *PDA Journal of Pharmaceutical Science and Technology* 1990; 44(2): 58-65.
16. Johnston TP, Punjabi MA, Froelich CJ. Sustained delivery of interleukin-2 from a poloxamer 407 gel matrix following intraperitoneal injection in mice. *Pharmaceutical research* 1992; 9(3): 425-434.
17. Miyazaki S, Ohkawa Y, Takada M, Attwood D. Antitumor Effect of Pluronic F-127 Gel Containing Mitomycin C on Sarcoma-180 Ascites Tumor in Mice. *Chemical and Pharmaceutical Bulletin* 1992; 40(8): 2224-2226.
18. Jeong B, Bae YH, Lee DS, Kim SW. Biodegradable block copolymers as injectable drug-delivery systems. *Nature* 1997; 388(6645): 860-862.
19. Tsitsilianis C. Responsive reversible hydrogels from associative "smart" macromolecules. *Soft Matter* 2010; 6(11): 2372-2388.
20. Zhang L, Eisenberg A. Multiple morphologies of" crew-cut" aggregates of polystyrene-b-poly (acrylic acid) block copolymers. *Science* 1995; 268(5218): 1728.
21. Ishihara K, Ueda T, Nakabayashi N. Preparation of phospholipid polymers and their properties as polymer hydrogel membranes. *Polymer Journal* 1990; 22(5): 355-360.
22. Zhang B. A possible connection between fast radio bursts and Gamma-ray bursts. *The Astrophysical Journal Letters* 2013; 780(2): L21.
23. Aikawa T, Konno T, Takai M, Ishihara K. Spherical phospholipid polymer hydrogels for cell encapsulation prepared with a flow-focusing microfluidic channel device. *Langmuir* 2011; 28(4): 2145-2150.
24. Ishihara K, Xu Y, Konno T. Cytocompatible Hydrogel Composed of Phospholipid Polymers for Regulation of Cell Functions. In: Kunugi S, Yamaoka, eds. *Polymers in Nanomedicine*. Springer, 2012: 141-165.

25. Oda H, Konno T, Ishihara K. The use of the mechanical microenvironment of phospholipid polymer hydrogels to control cell behaviour. *Biomaterials* 2013; 34(24): 5891-5896.
26. Salvage JP, Rose SF, Phillips GJ, Hanlon GW, Lloyd AW, Ma IY, Armes SP, Billingham NC, Lewis AL. Novel biocompatible phosphorylcholine-based self-assembled nanoparticles for drug delivery. *Journal of Controlled Release* 2005; 104: 259-270.
27. Salvage JP, Thom C, Lewis AL, Phillips GJ, Lloyd AW. Nanoprecipitation of polymeric nanoparticle micelles based on 2-methacryloyloxyethyl phosphorylcholine (MPC) with 2-(diisopropylamino)ethyl methacrylate (DPA), for intracellular delivery applications. *Journal of Materials Science: Materials in Medicine* 2015; 26: 150
28. Salvage JP, Smith T, Lu T, Sanghera A, Standen G, Tang Y, et al. Synthesis, characterisation, and in vitro cellular uptake kinetics of nanoprecipitated poly (2-methacryloyloxyethyl phosphorylcholine)-b-poly (2-(diisopropylamino) ethyl methacrylate)(MPC-DPA) polymeric nanoparticle micelles for nanomedicine applications. *Applied Nanoscience* 2016; 6: 1-22.
29. Ueda T, Oshida H, Kurita K, Ishihara K, Nakabayashi N. Preparation of 2-methacryloyloxyethyl phosphorylcholine copolymers with alkyl methacrylates and their blood compatibility. *Polymer Journal* 1992; 24: 1259-1269.
30. Ishihara K, Takai M. Bioinspired interface for nanobiodevices based on phospholipid polymer chemistry. *Journal of the Royal Society Interface* 2009; 6(Suppl 3): S279-S91.
31. Iwasaki Y, Ishihara K. Cell membrane-inspired phospholipid polymers for developing medical devices with excellent biointerfaces. *Science and Technology of Advanced Materials* 2012; 13: 14
32. Lewis AL. Phosphorylcholine-based polymers and their use in the prevention of biofouling. *Colloids and Surfaces B: Biointerfaces*. 2000; 18(3): 261-275.
33. Castelletto V, Hamley IW, Ma Y, Bories-Azeau X, Armes SP, Lewis AL. Microstructure and physical properties of a pH-responsive gel based on a novel biocompatible ABA-type triblock copolymer. *Langmuir*. 2004; 20(10): 4306-4309.
34. Yoshikawa HY, Rossetti FF, Kaufmann S, Kaindl T, Madsen J, Engel U, Lewis AL, Armes SP, and Tanaka M. Quantitative Evaluation of Mechanosensing of Cells on Dynamically Tunable Hydrogels. *Journal of the American Chemical Society* 2011; 133(5): 1367-1374.

35. Monzel C, Veschgini M, Madsen J, Lewis AL, Armes SP, Tanaka M. Fine Adjustment of Interfacial Potential between pH-Responsive Hydrogels and Cell-Sized Particles. *Langmuir* 2015; 31(31): 8689-8696.
36. Li C, Buurma NJ, Haq I, Turner C, Armes SP, Castelletto V, et al. Synthesis and characterization of biocompatible, thermoresponsive ABC and ABA triblock copolymer gelators. *Langmuir*. 2005; 21(24): 11026-11033.
37. O'Lenick TG, Jiang X, Zhao B. Thermosensitive Aqueous Gels with Tunable Sol− Gel Transition Temperatures from Thermo-and pH-Responsive Hydrophilic ABA Triblock Copolymer. *Langmuir* 2010; 26(11): 8787-8796.
38. Lee ALZ, Ng VWL, Gao S, Hedrick JL, Yang YY. Injectable Hydrogels from Triblock Copolymers of Vitamin E-Functionalized Polycarbonate and Poly (ethylene glycol) for Subcutaneous Delivery of Antibodies for Cancer Therapy. *Advanced Functional Materials* 2014; 24(11): 1538-1550.
39. Jeong B, Bae YH, Kim SW. Drug release from biodegradable injectable thermosensitive hydrogel of PEG–PLGA–PEG triblock copolymers. *Journal of controlled release*. 2000; 63(1): 155-163.
40. Joint Formulary Committee, 2015. British National Formulary. 70. London: BMJ Group and Pharmaceutical Press
41. Dominguez A, Fernandez A, Gonzalez N, Iglesias E, and Montenegro L. Determination of Critical Micelle Concentration of Some Surfactants by Three Techniques. *Journal of Chemical Education* 1997; 74(10): 1227-1231.
42. Shah VP, Tsong Y, Sathe P, Liu JP. In vitro dissolution profile comparison--statistics and analysis of the similarity factor, f2. *Pharmaceutical Research* 1998; 15(6): 889-896.
43. Shah VP, Tsong Y, Sathe P, Williams RL. Dissolution profile comparison using Similarity factor, f2. *Dissolution Technologies* 1999; 6(3): 1.
44. Costa P, Lobo JMS, Modeling and comparison of dissolution profiles. *European journal of pharmaceutical sciences* 2001; 13(2): 123-133.
45. Dash S, Murthy PN, Nath L, Chowdhury P. Kinetic modelling on drug release from controlled drug delivery systems. *Acta Poloniae Pharmaceutica* 2010; 67(3): 217-223.
46. Nochos A, Douroumis D, Bouropoulos N. In vitro release of bovine serum albumin from alginate/HPMC hydrogel beads. *Carbohydrate Polymers* 2008; 74(3): 451-457.

47. Al-Hamidi H, Edwards AA, Mohammad MA, Nokhodchi A. To enhance dissolution rate of poorly water-soluble drugs: Glucosamine hydrochloride as a potential carrier in solid dispersion formulations. *Colloids and Surfaces B: Biointerfaces* 2010; 76(1): 170-178.
48. Chi SC, Jun HW. Release rates of ketoprofen from poloxamer gels in a membraneless diffusion cell. *Journal of pharmaceutical sciences*. 1991; 80(3): 280-283.
49. Vroom, J. M., De Grauw, K. J., Gerritsen, H. C., Bradshaw, D. J., Marsh, P. D., Watson, G. K., Allison, C. Depth Penetration and Detection of pH Gradients in Biofilms by Two-Photon Excitation Microscopy. *Applied and Environmental Microbiology* 1999; 65(8): 3502–3511.
50. Liu J, Huang Y, Kumar A, Tan A, Jin S, Mozhi A, Liang XJ. pH-sensitive nanosystems for drug delivery in cancer therapy. *Biotechnology advances* 2014; 32(4): 693-710.
51. Blasi P, Schoubben A, Giovagnoli S, Perioli L, Ricci M, Rossi C. Ketoprofen poly(lactide-co-glycolide) physical interaction. *AAPS PharmSciTech* 2007; 8(2): E78-E85.
52. Chawla G, Bansal AK. Improved dissolution of a poorly water soluble drug in solid dispersions with polymeric and non-polymeric hydrophilic additives. *Acta Pharmaceutica* 2008; 58(3): 257-274.
53. Aguiar J, Carpena P, Molina-Bolıvar JA, Ruiz CC. On the determination of the critical micelle concentration by the pyrene 1: 3 ratio method. *Journal of Colloid and Interface Science* 2003; 258(1): 116-122.
54. Tew GN, Bhatia SR. PLA–PEO–PLA Hydrogels and Their Mechanical Properties. In: Bhatia SK, eds. *Engineering Biomaterials for Regenerative Medicine*. Springer, 2012: 127-140.
55. Lee AS, Bütün V, Vamvakaki M, Armes SP, Pople JA, Gast AP. Structure of pH-dependent block copolymer micelles: charge and ionic strength dependence. *Macromolecules* 2002; 35(22): 8540-8551.
56. Bohrey S, Chourasiya V, Pandey A. Polymeric nanoparticles containing diazepam: preparation, optimization, characterization, in-vitro drug release and release kinetic study. *Nano Convergence* 2016; 3(1): 1.
57. Taktak FF, Bütün V. Synthesis and physical gels of pH-and thermo-responsive tertiary amine methacrylate based ABA triblock copolymers and drug release studies. *Polymer* 2010; 51(16): 3618-3626.
58. Ysambertt, F., Vejar, F., Paredes, J., & Salager, J. L. The absorbance deviation method: a spectrophotometric estimation of the critical micelle concentration (CMC) of ethoxylated alkylphenol

surfactants. *Colloids and Surfaces A: Physicochemical and Engineering Aspects* 1998; 137(1-3): 189-196.

59. Singh V, Khullar P, Dave PN, Kaur N. Micelles, mixed micelles, and applications of polyoxypropylene (PPO)-polyoxyethylene (PEO)-polyoxypropylene (PPO) triblock polymers. *International Journal of Industrial Chemistry* 2013; 4(1): 1-18.
60. Frindi M, Michels B, Zana R. Ultrasonic absorption studies of surfactant exchange between micelles and bulk phase in aqueous micellar solutions of nonionic surfactants with a short alkyl chain. 3. Surfactants with a sugar head group. *The Journal of Physical Chemistry* 1992; 96(20): 8137-8141.
61. Zana R, Levy H, Kwetkat K. Mixed micellization of dimeric (gemini) surfactants and conventional surfactants. I. Mixtures of an anionic dimeric surfactant and of the nonionic surfactants C 12 E 5 and C 12 E 8. *Journal of colloid and interface science* 1998; 197(2): 370-376.
62. Regev O, Zana R. Aggregation behavior of tyloxapol, a nonionic surfactant oligomer, in aqueous solution. *Journal of colloid and interface science* 1999; 210(1): 8-17.
63. Pearson RT, Warren NJ, Lewis AL, Armes SP, Battaglia G. Effect of pH and Temperature on PMPC–PDPA Copolymer Self-Assembly. *Macromolecules* 2013; 46(4): 1400-1407
64. Robertson JD, Yealland G, Avila-Olias M, Chierico L, Bandmann O, Renshaw SA, Battaglia G. pH sensitive tubular polymersomes: Formation and applications in cellular delivery. *ACS Nano* 2014; 8(5): 4650-4661.

Tables

Table 1 Molecular weight (Mn and Mw) and polydispersity (Mw/Mn) of DPA_{50}-MPC_{250}-DPA_{50} triblock copolymer determined *via* ^{1}H NMR and organic GPC

DPA_{50}-MPC_{250}-DPA_{50}	Mn	Mw	Mw/Mn
Target ($g.mol^{-1}$)	95150	-	-
^{1}H NMR	95150	-	-
GPC	89030	89480	1.01

Table 2 Model-dependant analysis of the keto and spiro release profiles, displaying the coefficient of determination R^2 values, where R^2 > was indicative of good fit, together with the zero order (K_0), first order (K_1), and Higuchi (K_H) rate constants (K)

		Zero order K_0 rate constant			First order K_1 rate constant			Higuchi K_H rate constant		
	Time (hours)	0-32	0-8	24-32	0-32	0-8	24-32	0-32	0-8	24-32
Keto	R^2	0.189	0.420	0.999	0.880	0.844	0.899	0.342	0.701	0.998
	K	0.799	7.551	0.045	-0.066	-0.189	-0.112	7.121	29.732	0.479
Keto + gel	R^2	0.343	0.615	0.963	0.724	0.898	0.967	0.529	0.867	0.968
	K	1.070	8.438	0.053	-0.026	-0.124	-0.005	8.812	30.521	0.558
Spiro	R^2	0.771	0.838	0.995	0.855	0.886	0.997	0.908	0.984	0.997
	K	1.023	4.252	0.689	-0.007	-0.024	-0.006	7.357	14.048	7.266
Spiro + gel	R^2	0.860	0.907	0.991	0.912	0.936	0.991	0.964	0.996	0.990
	K	1.033	3.545	0.611	-0.007	-0.019	-0.005	7.245	11.320	6.447
Keto (+ spiro)	R^2	0.232	0.489	0.962	0.866	0.813	0.975	0.399	0.768	0.966
	K	0.900	8.131	0.013	-0.068	-0.177	-0.032	7.818	31.060	0.136
Keto (+ spiro) + gel	R^2	0.395	0.665	0.994	0.495	0.757	0.994	0.585	0.900	0.995
	K	0.706	5.227	0.069	-0.005	-0.035	-0.001	5.629	18.539	0.724
Spiro (+ keto)	R^2	0.717	0.860	0.996	0.849	0.919	0.996	0.865	0.962	0.996
	K	1.356	6.423	0.642	-0.012	-0.042	-0.008	9.871	20.707	6.778
Spiro (+ keto) + gel	R^2	0.411	0.635	0.828	0.457	0.675	0.828	0.600	0.880	0.829
	K	0.387	2.705	0.010	-0.002	-0.014	-0.001	3.096	19.714	0.109

Table 3 Cumulative release (%) data at the 1, 8, 24, and 32 hour time points, illustrating the effects of gel loading, and drug-drug and polymer-drug interactions, upon drug release (Mean ± SD, n = 3)

	Cumulative release (%)			
Time point	1 hour	8 hours	24 hours	32 hours
keto	82.4 (± 2.8)	98.5 (± 0.3)	99.6 (± 0.7)	100.0 (± 0.4)
Keto + gel	57.9 (± 8.9)	92.1 (± 0.7)	94.8 (± 2.1)	95.3 (± 0.2)
Keto (+ spiro)	70.5 (± 3.3)	97.3 (± 0.3)	99.8 (± 0.7)	99.8 (± 0.8)
Keto (+ spiro) + gel	31.6 (± 11.3)	54.7 (± 0.2)	56.9 (± 0.5)	57.4 (± 0.3)
Spiro	16.0 (± 2.7)	39.1 (± 0.5)	47.3 (± 1.5)	52.9 (± 0.2)
Spiro + gel	9.5 (± 3.5)	31.0 (± 1.2)	41.5 (± 1.4)	46.0 (± 0.4)
Spiro (+ keto)	18.1 (± 6.9)	54.2 (± 0.7)	63.6 (±0.6)	69.0 (± 0.1)
Spiro (+ keto) + gel	11.5 (± 1.5)	29.2 (± 0.1)	31.0 (± 0.9)	31.1 (± 0.2)

Table 4 Particle size (D_h), polydispersity (Pd), and critical micelle concentration (CMC) of DPA_{50}-MPC_{250}-DPA_{50} copolymer solutions ([a]0.15 % and [b]1.5 % w/v) determined *via* DLS and pyrene fluorescence spectroscopy. (Mean ± SD, n = 3)

DPA_{50}-MPC_{250}-DPA_{50}	D_h (nm) [a]	Pd [a]	CMC^1 (mg ml^{-1}) [b]	CMC^2 (mg ml^{-1}) [b]	CMC^3 (mg ml^{-1}) [b]
pH 2.0	16.6 (± 6.2)	0.536 (± 0.026)	-	-	-
pH 7.5	63.0 (± 6.1)	0.257 (±0.013)	0.004 (± 0.055)	0.043 (± 0.021)	0.469 (± 0.011)

Figures

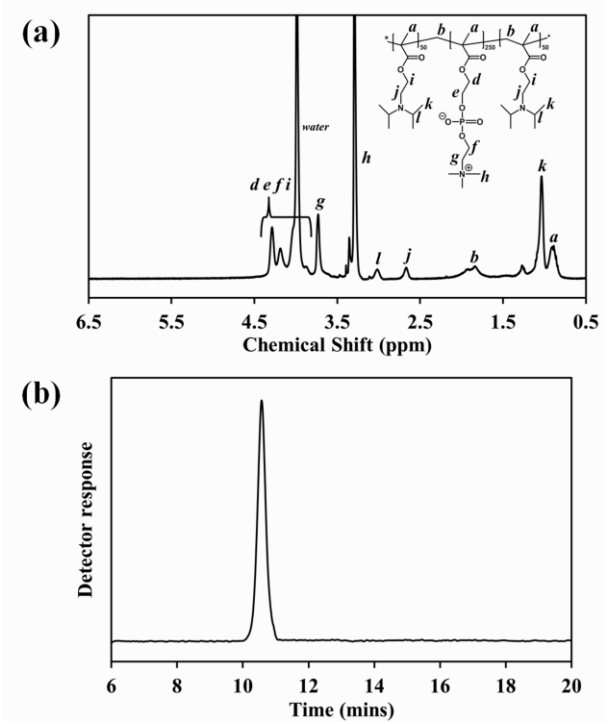

Figure 1 ^{1}H NMR spectra (a) and GPC elution profile (b) of DPA_{50}-MPC_{250}-DPA_{50} triblock copolymer

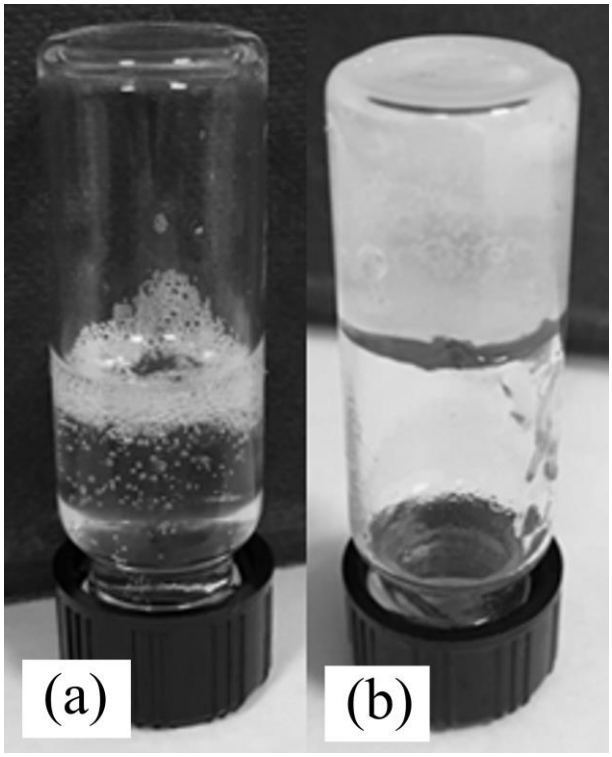

Figure 2 DPA_{50}-MPC_{250}-DPA_{50} 15 % w/v copolymer, illustrating the free-flowing solution at pH 2 (a) *versus* the free-standing gel formed at pH7.5 (b)

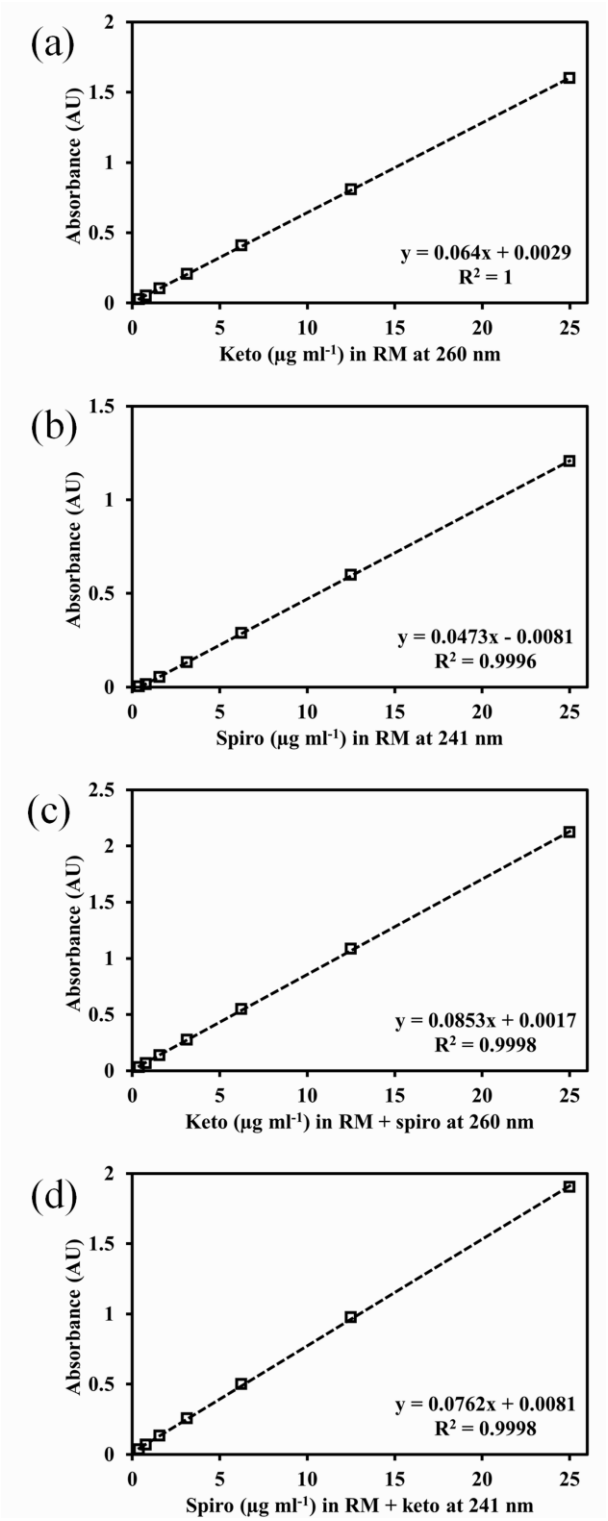

Figure 3 Standard curves of keto in RM (a), spiro in RM (b), keto in RM + spiro (c), and spiro in RM + keto (d) (Mean ± SD, n = 3)

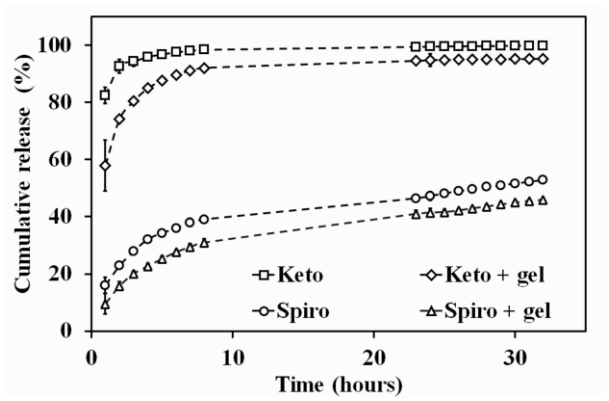

Figure 4 Individual cumulative drug release profiles of keto and spiro, in free solution, and from 15 % w/v DPA_{50}-MPC_{250}-DPA_{50} copolymer gel, in RM (pH 7.5) at 37 °C (Mean ± SD, n = 3)

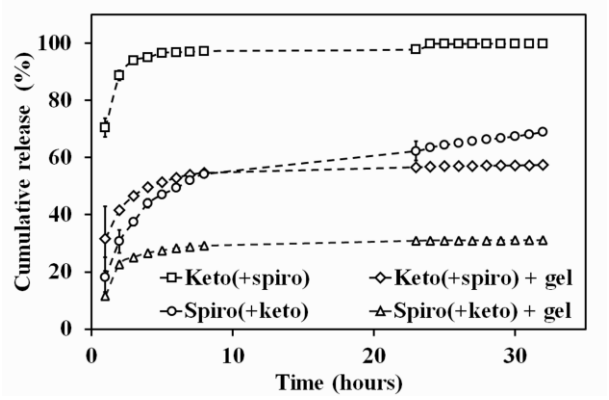

Figure 5 Combined cumulative drug release profiles of keto(+spiro) and spiro(+keto), in free solution, and from 15 % w/v DPA_{50}-MPC_{250}-DPA_{50} copolymer gel, in RM (pH 7.5) at 37 °C (Mean ± SD, n = 3)

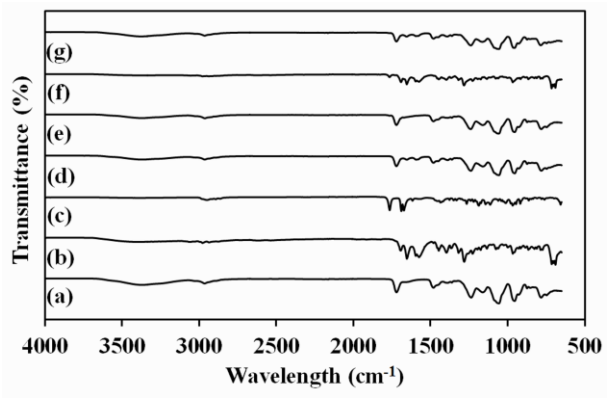

Figure 6 FTIR spectra of (a) copolymer, (b) keto, (c) spiro, (d) copolymer + keto, (e) copolymer + spiro, (f) keto + spiro, (g) copolymer + keto + spiro

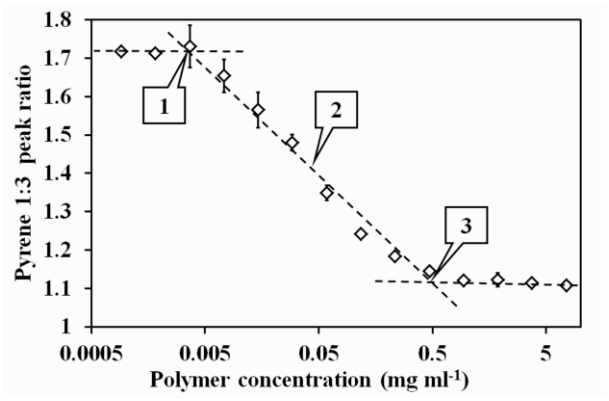

Figure 7 Critical micelle concentration of DPA_{50}-MPC_{250}-DPA_{50} at pH 7.5 determined by pyrene fluorescence spectrometry, indicating CMC^1, CMC^2, and CMC^3 (Mean ± SD, n = 3)

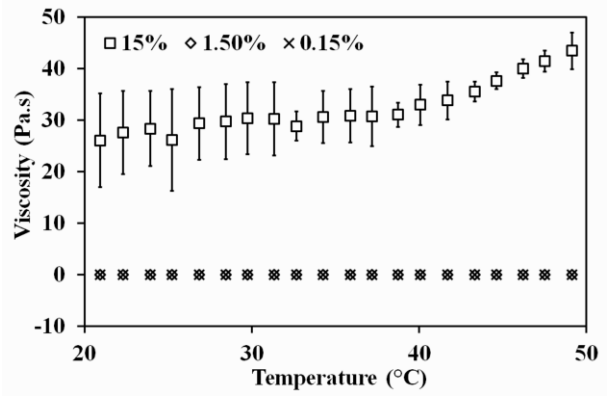

Figure 8 Temperature dependent (20 – 50 °C) viscosity (Pa.s) at 1 Pa oscillating stress, of 15, 1.5, and 0.15 % w/v DPA_{50}-MPC_{250}-DPA_{50} copolymer solutions (pH 7.5). (Mean ± SD, n = 3)

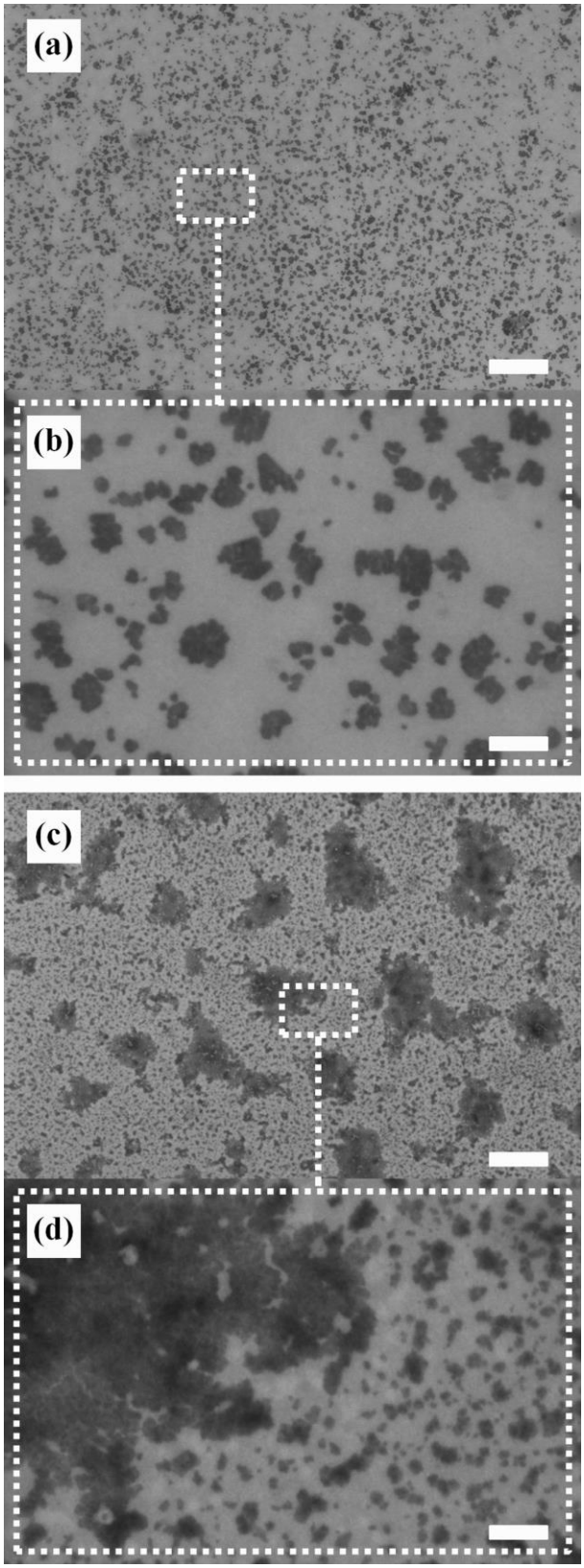

Figure 9 STEM images of 0.15 (a & b) and 1.5 (c & d) % w/v DPA_{50}-MPC_{250}-DPA_{50} copolymer solutions (pH 7.5), displaying wide area views of the polymer nanoparticles, and zoomed areas to highlight nanoparticle size and morphology. Scale bars = 600 nm and 100 nm for wide and zoom respectively.

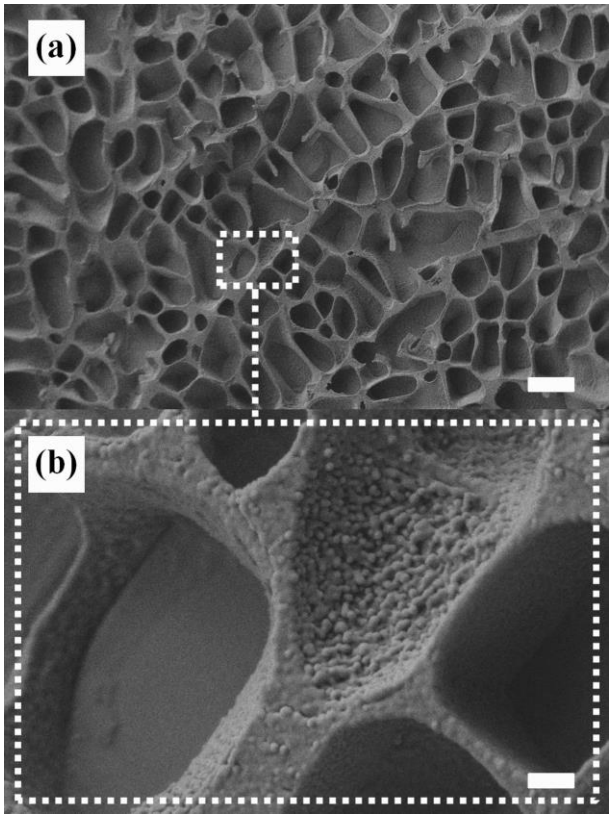

Figure 10 Cryo-SEM images of 15 % w/v DPA_{50}-MPC_{250}-DPA_{50} copolymer solution (pH 7.5), displaying a wide area view of the polymer gel matrix (a), and a zoomed area highlighting the nanostructured composition of the gel material (b). Scale bars = 4 µm and 400 nm for wide and zoom respectively.

In compliance with the Wiley self-archiving policy:

This is the peer reviewed version of the following article: [Azmy, B., Standen, G., Kristova, P., Flint, A., Lewis, A. L. and Salvage, J. P. (2017), Nanostructured DPA-MPC-DPA triblock copolymer gel for controlled drug release of ketoprofen and spironolactone. Journal of Pharmacy and Pharmacology. doi: 10.1111/jphp.12733], which has been published in final form at [http://dx.doi.org/10.1111/jphp.12733]. This article may be used for non-commercial purposes in accordance with Wiley Terms and Conditions for Self-Archiving.

http://onlinelibrary.wiley.com/wol1/doi/10.1111/jphp.12733/abstract

Publication History
Submitted/received: 23rd January 2017
Accepted: 26th March 2017
Published Online: 7th May 2017

In accordance with the Wiley self-archiving policy, there is a 12 months embargo on this document.